Fusion Engineering and Design xxx (xxxx) xxx–xxx

Contents lists available at ScienceDirect

Fusion Engineering and Design

journal homepage: www.elsevier.com/locate/fusengdes

Effects of TiC content on microstructure, mechanical properties, and thermal conductivity of W-TiC alloys fabricated by a wet-chemical method

Shaoting Lang[a,b], Qingzhi Yan[a,b,*], Ningbo Sun[a,b], Xiaoxin Zhang[a,b], Changchun Ge[a,b]

[a] Institute of Nuclear Materials, University of Science & Technology Beijing, 30 Xueyuan Road, Haidian District, Beijing 100083, China
[b] Beijing Municipal Key Lab for Advanced Energy Materials and Technologies, University of Science & Technology Beijing, 30 Xueyuan Road, Haidian District, Beijing 100083, China

ARTICLE INFO

Keywords:
W-TiC alloy
Wet-chemical method
Microstructure characterization
Mechanical properties
Thermal conductivities

ABSTRACT

W-(0–0.9)TiC (wt.%) alloys were prepared by a wet-chemical method and spark plasma sintering. The effects of TiC content on the microstructures, mechanical properties, and thermal conducting properties of the prepared W-TiC alloys were investigated. The results revealed that the average grain size of the W-(0–0.9)TiC alloys decreased, and their average TiC particle size increased with the increase of TiC content. The bending fracture strengths of the prepared samples increased significantly with increased TiC content in the range of 0–0.5%, which was attributed to the uniform distribution of TiC particles with a high proportion located in the tungsten grain interiors. The W-0.5TiC alloy exhibited the best mechanical properties with the highest relative density, bending strength, and flexural strain of 97.61%, 1065.72 MPa, and 1.23%, respectively. Moreover, the thermal conductivities of the W-(0.1–0.5)TiC alloys were slightly lower than those of pure tungsten at all testing temperatures. However, the mechanical properties and thermal conducting properties of the W-0.7TiC and W-0.9TiC alloys were significantly deteriorated due to the non-uniform aggregation of TiC particles at the tungsten grain boundaries.

1. Introduction

Tungsten (W), as a kind of refractory metal, possesses a high melting temperature of 3410 °C and high strength at elevated temperatures [1,2]. This makes tungsten an excellent candidate material for use in many important high temperature applications, such as kinetic energy penetrators [3], heating elements, critical components in rockets and missiles [4,5], and plasma-facing materials (PFMs) in future fusion reactors. However, there are drawbacks to tungsten, such as low-temperature brittleness, high-temperature or recrystallization brittleness, and irradiation induced brittleness and hardening [6–8], which limit the further applications of tungsten materials. In order to alleviate these problems, extensive researches have been carried out, and as a result, many tungsten alloys have been developed. Among these alloys, TiC particle reinforced tungsten alloy has been proved to be very promising due to its high bending strength, desirable impact ductility, excellent high temperature tensile strength, and outstanding irradiation resistance [9–13].

Recent studies here on W-TiC alloys, which are prepared by a wet-chemical method, showed that uniform core-shell structure (TiC_p/W) powders are obtained, that nano TiC particles are dispersed uniformly in tungsten matrixes with a high proportion located in grain interiors after sintering, and that W-TiC alloys are significantly strengthened by TiC particles [14,15]. Moreover, the W-TiC alloys also exhibits significantly improved mechanical properties and high temperature tensile properties as well as reduced ductile-to-brittle transition temperature after hot rolling [16]. This indicated that the wet-chemical method was effective for preparing W-TiC alloys with desirable properties. In this paper, the effects of TiC content on the microstructures, mechanical properties, and thermal conducting properties of the W-TiC alloys prepared by a wet-chemical method were examined. And as a base line, pure tungsten sample was also fabricated by the same method.

2. Experimental procedure

2.1. Powder preparation, reduction, and sintering

The detailed wet-chemical method with the addition of 1 wt.% polyvinylpyrrolidone (PVP, K30) to produce W-TiC alloys can be found in Ref. [15]. Ammonium metatungstate ($(NH_4)_6W_7O_{24}{\cdot}6H_2O$, AMT), hydrochloric acid, PVP, and nano TiC powders (average particle size, 50 nm; purity > 99%, Kaier Nano) were used in this investigation.

* Corresponding author at: Institute of Nuclear Materials, University of Science & Technology Beijing, 30 Xueyuan Road, Haidian District, Beijing, 100083, China.
E-mail address: qzyan@ustb.edu.cn (Q. Yan).

http://dx.doi.org/10.1016/j.fusengdes.2017.07.026
Received 5 October 2016; Received in revised form 24 June 2017; Accepted 31 July 2017

Table 1
The contents of raw materials used in the preparation of the W-(0–0.9)wt.%TiC precursor powders.

Sample	AMT (g)	TiC (g)	Deionized water (ml)	HCl solution (ml)	PVP (g)
PW	41.32	0	30	30	0
W-0.1TiC	41.32	0.03	30	50	0.3
W-0.3TiC	41.32	0.09	75	100	0.75
W-0.5TiC	41.32	0.15	125	150	1.25
W-0.7TiC	41.32	0.21	175	200	1.75
W-0.9TiC	41.32	0.27	225	250	2.25

Precursor powders of pure tungsten (PW) and W-TiC alloys with TiC content of 0.1, 0.3, 0.5, 0.7 and 0.9 wt.% were prepared via a wet-chemical method. The detailed contents of raw materials used in the preparation of each precursor powder are listed in Table 1. The higher content of TiC powders demanded that the contents of required deionized water and PVP be increased accordingly to facilitate the dispersion of TiC particles in solutions. The reduction process used a tube furnace in a high purity hydrogen atmosphere. The W-(0-0.9) TiC precursor powders were reduced at 600 °C for 2 h and at 800 °C for 0.5 h at a heating rate of 5 °C/min. Then the powders were cooled down naturally along with the furnace to room temperature (RT). The hydrogen flow rates were 0.2 L/min at RT–400 °C and 0.5 L/min at > 400 °C.

Spark plasma sintering was performed to consolidate the reduced powders under vacuum by using graphite dies. Powders were held at 1600 °C and 50 MPa for 1 min. The heating rate was 150 °C/min from RT to 700 °C, 80 °C/min from 700 °C to 1200 °C, and 150 °C/min from 1200 °C to 1600 °C. The size of the sintered samples was about 20 mm in diameter and 4.0–5.0 mm in thickness.

2.2. Characterization

The densities of the sintered samples were measured via the Archimedes method. The crystal structures were identified by X-ray diffraction (XRD). The mechanically ground and polished samples were subjected to Vickers micro-hardness tests with a loading weight of 200 g for 10 s. Specimens with dimensions of 3 × 2 × 16 mm were used to measure the fracture strength via a three point bending test at room temperature. The working span was 10 mm, and the constant loading rate was 0.5 mm/min. Field emission scanning electron microscopy (FESEM, Zeiss Ultra 55 and 450) equipped with a BSED (backscattered-electron diffraction) detector were performed to characterize the morphologies of the powders, sintered samples, and fracture surfaces. The average grain size and second phase particle size were statistically analyzed using quantitative metallography based on more than 200 grains and 500 particles, respectively, from the BSED-SEM images of the sintered samples. The oxygen and nitrogen contents of the sintered samples were measured by an ON-3000 analyzer, and the sulfur contents were measured by a CS-3000 analyzer. The thermal conductivities (λ) of the sintered samples were calculated from the thermal diffusivity (α), specific heat (C_p), and density (ρ) by the following formula:

$$\lambda = \alpha \cdot C_p \cdot \rho$$

The specific heat (C_p) was measured by a thermal analyzing apparatus (Dupont 1090B, America). The thermal diffusivity (α) was determined using a laser flash apparatus (LFA 457, Germany). The testing temperatures were in the range of RT to 800 °C.

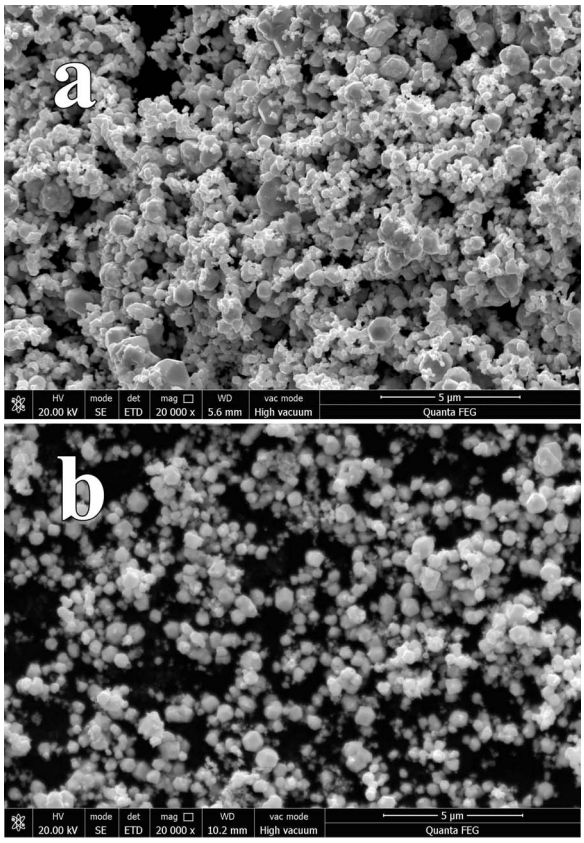

Fig. 1. FESEM images of the reduced (a) PW powder and (b) typical W-TiC alloy powders.

3. Results and discussion

3.1. Microstructure

Fig. 1 shows the FESEM images of the reduced PW powder and typical W-0.5TiC alloy powders. It can be noticed that the PW powders (Fig. 1(a)) displayed an aggregated morphology with primary particle sizes in the range of 0.1–1.2 µm and an average particle size of about 0.6 µm. From the typical FESEM image of the prepared W-0.5TiC alloy powders (Fig. 1(b)), it can be noticed that they displayed a slightly aggregated morphology with primary particle sizes in the range of 0.1–1.0 µm and an average particle size of about 0.5 µm. And the other reduced W-TiC alloy powders all showed similar particle morphologies and sizes to those of the W-0.5TiC alloy powders. The differences between the PW powders and the W-TiC alloy powders were attributed to their different chemical precipitation processes. As suspended TiC particles in solution acted as precipitate nuclei, this was a precipitate-coating process in which precipitates uniformly coated the surfaces of TiC particles during the preparation of the W-TiC precursors. Combined with the dispersing effect of PVP, this led to fine particle sizes in the precipitates and hence fine particle sizes in the final W-TiC particles. However, it was a pure precipitation process for tungstic acid ($WO_3 \cdot H_2O$) in solution and happened without a dispersing agent (PVP) during the preparation of the PW precursor. This resulted in large precipitate particle sizes and particle aggregation in the PW powders. Furthermore, the similar particle morphologies and sizes of the other W-TiC alloy powders were attributed to the same chemical precipitate coating and hydrogen reduction processes.

XRD patterns of the sintered PW and W-(0.1–0.9)TiC alloys are shown in Fig. 2. All diffraction peaks of the PW sample and the W-(0.1–0.7)TiC alloys were consistent with the standard pure tungsten (JCPDS#04-0806). No TiC peaks were detected in the XRD patterns of the W-(0.1–0.7)TiC alloys because of the low TiC proportions. However,